

Article

## Glycine Betaine Recognition through Cation– $\pi$ Interactions in Crystal Structures of Glycine Betaine Complexes with C-Ethyl-pyrogallol[4]arene and C-Ethyl-resorcin[4]arene as Receptors

Ikuhide Fujisawa<sup>1,\*</sup> and Katsuyuki Aoki<sup>2,\*</sup>

<sup>1</sup> Department of Environmental and Life Sciences, Toyohashi University of Technology, Hibarigaoka 1-1, Tempakucho, Toyohashi, Aichi 441-8580, Japan

<sup>2</sup> Department of Materials Science, Toyohashi University of Technology, Hibarigaoka 1-1, Tempakucho, Toyohashi, Aichi 441-8580, Japan

\* Authors to whom correspondence should be addressed; E-Mails: ifujisawa@ens.tut.ac.jp (F.I.); kaoki@tutms.tut.ac.jp (A.K.); Tel.: +81-532-44-6819 (F.I.); Fax: +81-532-48-5833 (F.I.).

Received: 21 January 2013; in revised form: 7 March 2013 / Accepted: 25 March 2013 /

Published: 16 April 2013

---

**Abstract:** The glycine betaine (betaine), interacts with several types of proteins with diverse structures *in vivo*, and in the contact regions, the aromatic rings of protein residues are frequently found beside the trimethylammonium group of betaine, implying the importance of the cation– $\pi$  interactions in recognition of this molecule. The crystal structures determined by X-ray crystallography of the complexes of betaine and C-ethyl-pyrogallol[4]arene (pyrogallol cyclic tetramer: PCT) and betaine and C-ethyl-resorcin[4]arene (resorcinol cyclic tetramer: RCT) mimic the conformations of betaine and protein complexes and show that the clathrate conformations are retained by the cation– $\pi$  interactions. The difference of the conformation feature of betaine in the Protein Data Bank and in the Cambridge Structural Database was found by chance during the research and analyzed with the torsion angles.

**Keywords:** betaine; cation– $\pi$  interactions; trimethylammonium group; aromatic rings; probable conformations

---

## 1. Introduction

Betaine is synthesized *in vivo* through two subsequent oxidation steps from choline [1]. In the rat liver, the first step is catalyzed by electron transfer-linked choline dehydrogenase in mitochondria [2,3] and the next step by nicotinamide adenine dinucleotide (NAD)-dependent betaine-aldehyde dehydrogenase. Betaine-homocysteine-S-methyltransferase (E.C. 2.1.1.5) requires betaine together with zinc ion as an important methyl donor coenzyme for metabolizing homocysteine, which is one of the inductive factors of atherosclerosis, to methionine in liver and kidney of man and pig [4–7]. Betaine is a simple small molecule composed of a methylene group with a cationic trimethylammonium group and a carboxyl group at both ends. The structural flexibility of non-hydrogen atoms in the molecule is limited at two torsion angles around two bonds of a methylene group.

In the Protein Data Bank (PDB), the structures of 13 kinds of proteins with betaine molecules are revealed [8–20], and in the almost structures, aromatic rings of protein amino acids interact with the trimethylammonium group of betaine through cation– $\pi$  interaction, except for two structures. In many kinds of protein architectures recognizing molecules with trimethylammonium groups, the cation– $\pi$  interactions play important roles for recognition and binding [21,22]. In the Cambridge Structural Database (CSD), just one betaine structure among about one hundred fifteen reported betaine structures seems to form the cation– $\pi$  interaction, though it is not clear whether the cation– $\pi$  interaction is critical for the structure formation, because many other hydrogen bonds are formed simultaneously.

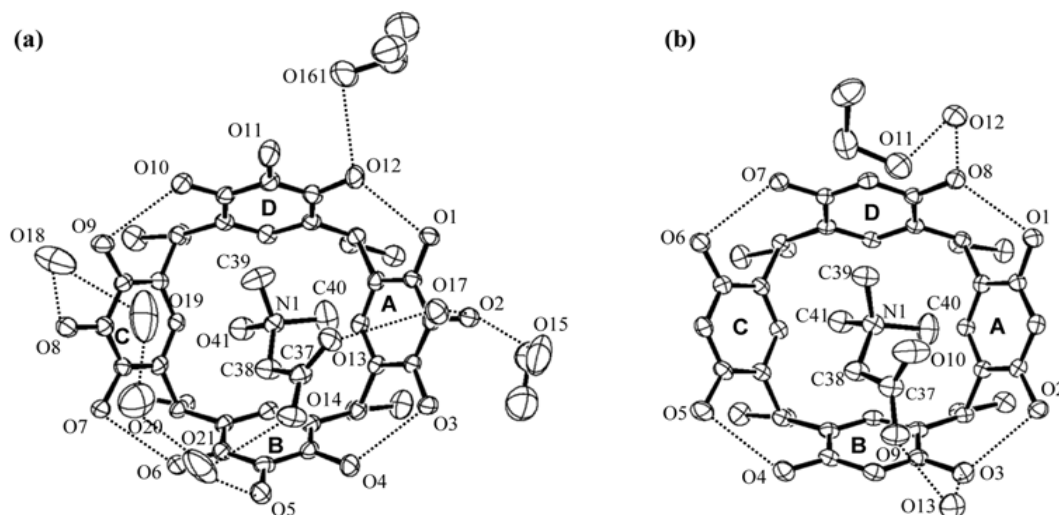
In this research, the two structures, betaine-C-ethyl-pyrogallol[4]arene (pyrogallol cyclic tetramer: PCT) and betaine-C-ethyl-resorcin[4]arene (resorcinol cyclic tetramer: RCT), in which the trimethylammonium group is bound, mainly by cation– $\pi$  interactions, are solved with X-ray crystallography.

## 2. Results and Discussion

PCT and RCT are the artificially synthesized cyclic tetramers, which are often used to investigate the cation– $\pi$  interactions [23]. The crystals of the PCT-betaine complex and the RCT-betaine complex were obtained from each solution in ethanol and water at room temperature. The PCT-betaine structure and the RCT-betaine structure were determined by X-ray crystallography with the data measured at 120 K and 107 K, respectively.

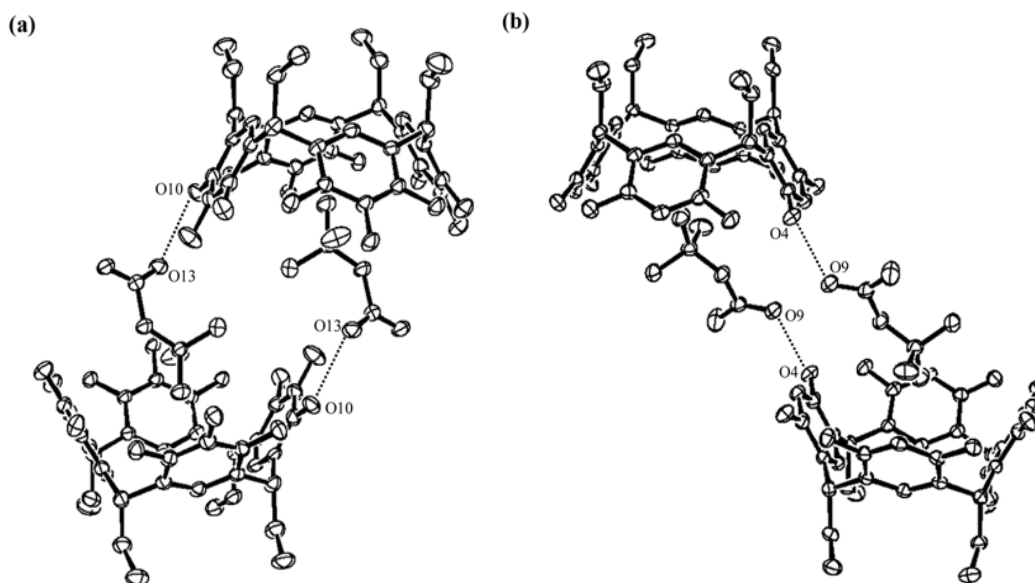
In each crystal structure, a betaine molecule makes a complex with a cyclic tetramer molecule. The trimethylammonium group of the betaine molecule faces toward the bottom of the aromatic bowl of the cyclic tetramer molecule. The conformation of betaine and the relative position to PCT or RCT in each complex are similar to each other (Figure 1). The trimethylammonium group of betaine is in the distance to form cation– $\pi$  interactions with aromatic rings of PCT or RCT. No conventional hydrogen bond with the trimethylammonium group is observed. Almost only cation– $\pi$  interactions keep the position of the trimethylammonium group fixed, indicating its importance for the structural formations of complexes.

**Figure 1.** The structures of betaine complexes with pyrogallol cyclic tetramer (PCT) (a) and resorcinol cyclic tetramer (RCT); (b) determined by X-ray crystallography are described with ORTEP. Dotted lines represent conventional hydrogen bonds. The names of all oxygen atoms and atoms of the betaine molecule are indicated to distinguish the atoms. Distances (Å) from the carbon atoms of the trimethylammonium group of betaine to the  $\pi$ -centroids of PCT ( $< 4.1$  Å): C40...ring A = 3.16, C41...ring B = 3.56, C41...ring C = 3.34 and C41...ring D = 3.87 and to the  $\pi$ -centroids of RCT ( $< 4.1$  Å): C40...ring A = 3.32, C41...ring B = 3.90, C41...ring C = 3.50 and C41...ring D = 3.71.



Both complexes are composed of an equimolar of betaine and PCT or betaine and RCT, and each two upside-down complexes make a pair (Figure 2). The crystal structures, including tetramethylammonium, analogous molecules to betaine, complexed with the cyclic tetramer, PCT or RCT have been solved and reported as CSD ID of JALFEI [24], PUJQOA [25], XUSZUG [26], XUTBAP [26], XUSZOA [26] and UKERIL [27]. Except for UKERIL, two molecules upside-down to each other of PCT or RCT form an almost complete capsule-like structure sandwiching solvent molecules between them, in some cases, with the complex ratio of the cyclic tetramer and tetramethylammonium of 2:1. Compared with these structures, the complex structures, including betaine, could not form complete capsule-like structures and take the laterally slid complex pair structures, because of the carboxyl group of betaine. In both complexes, two upside-down PCT or RCT molecules did not form direct hydrogen bonds to each other, while betaine molecules form hydrogen bonds to PCT or RCT molecules in the counterpart complexes, shaping the laterally slid complex pair structures. The way of coupling the complexes is different between PCT and RCT. The upside-down complexes make not a complete capsule, but a disturbed complex pair slid laterally in the direction for two betaine carboxyl groups becomes far in the PCT-betaine structure and near in the RCT-betaine structure. This may be caused by electrostatic repulsion between the carboxyl group of betaine and the one more hydroxyl group per aromatic ring of PCT than of RCT.

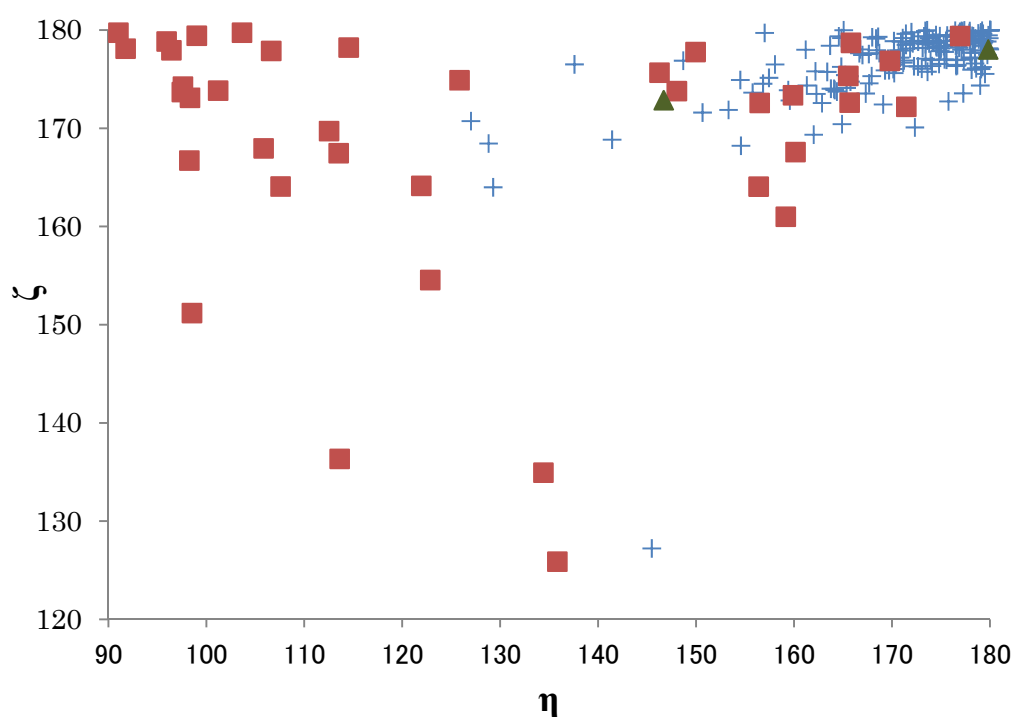
**Figure 2.** The slid complex pair structures composed of two complexes. One complex is composed (a) of a betaine molecule and a PCT molecule; and (b) of a betaine molecule and a RCT molecule. Ethanol and water molecules are not drawn for clarity. Hydrogen bonds between two complexes are represented by dotted lines. Each upside-down structure is positioned with crystallographic symmetry. It is inferred that one more hydroxyl group per aromatic ring of PCT compared to RCT prevents the PCT complex from forming the same structure as the RCT complex.



Many betaine structures have already been determined and reported as small organic chemicals in CSD and as ligands to proteins in PDB. Interestingly, the distributions of the conformations are different between CSD and PDB. To describe the structural distribution, two torsion angles around the methylene group, which are only flexible parts of non-hydrogen atoms in betaine structures, were measured. The absolute value of the torsion angle around the bond between the methylene group and the carboxyl group was named  $\eta$ , and the absolute value of the torsion angle around the bond between the methylene group and the trimethylammonium group was named  $\zeta$ . The distribution was drawn in Figure 3. The angles,  $\eta$ , of the structures in CSD are over  $120^\circ$ , while in PDB, those range around  $90^\circ$  to  $180^\circ$ ; about one third of them are between  $90^\circ$  and  $110^\circ$ , and the other third are over  $150^\circ$ . The angles,  $\zeta$ , are nearly unchanged values,  $180^\circ$  in both CSD and PDB, except for a few cases. The result of a brief simulation with Chem3D (PerkinElmer Inc., Waltham, MA, USA) shows that the conformation is most stable when the angle,  $\eta$ , is  $90^\circ$ , while the result with CONFLEX (CONFLEX Co., Shinagawa, Tokyo, Japan) shows that the conformation with the highest probability occurs when the angle,  $\eta$ , is  $180^\circ$  for the non-ionization form of the carboxyl group,  $-\text{COOH}$ , and when the angle,  $\eta$ , is  $90^\circ$  for the ionization form,  $-\text{COO}^-$ . The angles,  $\eta$ , of the PCT-betaine and RCT-betaine complexes are about  $180^\circ$  and  $150^\circ$ , respectively. These values are in the range that the angles,  $\eta$ , of most betaine structures reported in CSD fall within. The angles,  $\zeta$ , in PCT and RCT complex structures are both about  $180^\circ$ , showing the same tendency as the other small molecule complexes in CSD. This  $\eta$  and  $\zeta$  analysis shows that the betaine molecules, which mainly interact through the cation- $\pi$  interactions

with host molecules, PCT or RCT, have similar structures to the structures reported in CSD and to the one third group of the structures reported in PDB.

**Figure 3.** The absolute values of torsion angles of betaine structures reported in CSD (+), in PDB (■) and here (▲). The almost  $\zeta$  values are seen between  $160^\circ$  and  $180^\circ$ , both in CSD and PDB, while the tendency of the distribution of the  $\eta$  values are different. The  $\eta$  values observed in CSD structures are almost over  $150^\circ$ , especially gathered near  $180^\circ$ . The  $\eta$  values observed in PDB structures can fall into three groups; the first group is between  $90^\circ$  and  $110^\circ$ , the second between  $110^\circ$  and  $150^\circ$  and the third group over  $150^\circ$ . The third group has the similar tendency of distribution as the structures in CSD. The structures determined here are categorized into the third group.



### 3. Experimental Section

PCT and RCT compound was synthesized by an analogous method [28]. The PCT-betaine complex was crystallized from the solution mixing betaine aqueous solution (0.5 mol/L, 1.0 mL), PCT ethanol solution (0.05 mol/L, 2.0 mL), ethanol (1.0 mL) and water (1.0 mL) with evaporation at room temperature for about two weeks. The RCT-betaine complex was crystallized from the solution mixing betaine aqueous solution (0.5 mol/L, 0.2 mL), RCT ethanol solution (0.05 mol/L, 2.0 mL), ethanol (3.0 mL) and water (1.8 mL) with evaporation at room temperature for about three weeks. Each crystal used for X-ray diffraction experiments was  $0.4 \times 0.4 \times 0.1$  mm and  $0.4 \times 0.3 \times 0.05$  mm in size for PCT-betaine and RCT-betaine, respectively. Both crystals are orange platelets.

The diffraction experiments were made on a Rigaku AFC-7R diffractometer with graphite-monochromated Mo  $K\alpha$  radiation ( $\lambda = 0.71069$  Å) using a rotating anode generator and a Mercury CCD camera at cryo-condition, 120 K for PCT-betaine and 107 K for RCT-betaine. Data reduction, cell refinement and semi-empirical absorption correction was performed with the program

CrystalClear (Rigaku Co., Akishima, Tokyo, Japan). The solution of the initial structure by the direct method and refinement of the model by full-matrix least-squares methods, minimizing the function  $\sum w(|F_o| - |F_c|)^2$ , were executed with the program, SHELXS and SHELXL [29], respectively, on the platform and graphic software, Yadokari-XG [30].

Crystal data for PCT•betaine•2EtOH•5H<sub>2</sub>O: C<sub>43</sub>H<sub>69</sub>NO<sub>21</sub>, fw = 964.04, triclinic, space group  $P - 1$ ,  $a = 12.0178(16)$ ,  $b = 12.275(2)$ ,  $c = 17.554(3)$  Å,  $\alpha = 109.887(4)$ ,  $\beta = 91.042(2)$ ,  $\gamma = 101.332(3)^\circ$ ,  $V = 2377.4(6)$  Å<sup>3</sup>,  $Z = 2$ ,  $D_{\text{calcd}} = 1.347$  g cm<sup>-3</sup>,  $\mu(\text{Mo K}\alpha) = 1.06$  cm<sup>-1</sup>,  $F(000) = 1,036$ . All non-hydrogen atoms were refined with anisotropic temperature factors. The positions of hydrogen atoms, except water molecules, were determined and refined with the riding mode. All distances and angles between non-hydrogen atoms in ethanol models are restrained explicitly. The oxygen atom in one ethanol molecule was refined as an atom disordered to two positions. Final  $RI = 0.0925$ ,  $wR2 = 0.2501$  (for 6,754 reflections with  $I > 2\sigma(I)$  out of 9,860 unique in the range  $4 < 2\theta < 54^\circ$ ) and  $GOF = 1.146$ .

Crystal data for RCT•betaine•EtOH•2H<sub>2</sub>O: C<sub>43</sub>H<sub>61</sub>NO<sub>13</sub>, fw = 799.93, triclinic, space group  $P - 1$ ,  $a = 12.1241(15)$ ,  $b = 13.3655(19)$ ,  $c = 13.964(2)$  Å,  $\alpha = 86.356(15)$ ,  $\beta = 82.010(15)$ ,  $\gamma = 73.242(10)^\circ$ ,  $V = 2,145.1(5)$  Å<sup>3</sup>,  $Z = 2$ ,  $D_{\text{calcd}} = 1.238$  g cm<sup>-3</sup>,  $\mu(\text{Mo K}\alpha) = 0.91$  cm<sup>-1</sup>,  $F(000) = 860$ . All non-hydrogen atoms were refined with anisotropic thermal parameters. The positions of hydrogen atoms were determined and refined with the riding mode, except hydrogen atoms of water molecules, whose positions were determined with difference Fourier peaks and refined without restraints. Final  $RI = 0.0722$ ,  $wR2 = 0.1967$  (for 7,067 reflections with  $I > 2\sigma(I)$  out of 8,883 unique in the range  $4 < 2\theta < 54^\circ$ ) and  $GOF = 1.090$ .

Figures with temperature factors were drawn with the ORTEP32 program [31]. The structures were deposited to the Cambridge Structural Database Centre after checking with the program, enCIFer. Crystallographic data have been deposited with the Cambridge Crystallographic Data Centre as supplementary publication Nos. CCDC 916650 and CCDC 916651 for the PCT-betaine complex and the RCT-betaine complex, respectively [32].

#### 4. Conclusions

This research shows that betaine can bind through cation- $\pi$  interactions with aromatic rings, as is similar to other complex structures having trimethylammonium groups, and that the carboxyl group addition on tetramethylammonium prevents the complex pair from forming entire capsule-like structures, inducing the laterally slid complex pair structures made from two cyclic tetramers upside-down to each other. The distributions of the betaine conformation are different between PDB structures and CSD structures. The structures reported in this work are similar to the CSD structures group and the one-third group of PDB structures. Because of the high resolution, the structures of small molecules mimicking macromolecules enable us to observe detailed points precisely, giving us a precise knowledge of the interaction and recognition conformation of proteins.

## Acknowledgments

The authors thank the Instrument Center of the Institute for Molecular Science in Okazaki for permission and advice on the usage of their X-ray diffractometer equipment. Also, the authors are deeply grateful to Y. Kitamura and R. Okamoto for the synthesis of the compounds, PCT and RCT.

## Conflict of Interest

The authors declare no conflict of interest.

## References and Notes

1. Landfald, B.; Strøm, A.R. Choline-glycine betaine pathway confers a high level of osmotic tolerance in *Escherichia coli*. *J. Bacteriol.* **1986**, *165*, 849–855.
2. Ebisuzaki, K.; Williams, J.N. Preparation and partial purification of soluble choline dehydrogenase from liver mitochondria. *Biochem. J.* **1955**, *60*, 644–646.
3. Tsuge, H.; Nakano, Y.; Onishi, H.; Futamura, Y.; Ohashi, K. A novel purification and some properties of rat liver mitochondrial choline dehydrogenase. *Biochim. Biophys. Acta* **1980**, *614*, 274–284.
4. Finkelstein, J.D.; Martin, J.J. Methionine metabolism in mammals. *J. Biol. Chem.* **1984**, *259*, 9508–9513.
5. Finkelstein, J.D.; Kyle, W.E.; Harris, B.J. Methionine metabolism in mammals. Regulation of homocysteine methyltransferases in rat tissue. *Arch. Biochem. Biophys.* **1971**, *146*, 84–92.
6. McKeever, M.P.; Weir, D.G.; Molloy, A.; Scott, J.M. Betaine-homocysteine methyltransferase: Organ distribution in man, pig and rat and subcellular distribution in the rat. *Clin. Sci.* **1991**, *81*, 551–556.
7. DiBello, P.M.; Dayal, S.; Kaveti, S.; Zhang, D.; Kinter, M.; Lentz, S.R.; Jacobsen, D.W. The nutrigenetics of hyperhomocysteinemia. *Mol. Cell. Proteomics* **2010**, *9*, 471–485.
8. Schiefner, A.; Breed, J.; Bösser, L.; Kneip, S.; Gade, J.; Holtmann, G.; Diederichs, K.; Welte, W.; Bremer, E. Cation- $\pi$  interactions as determinants for binding of the compatible solutes glycine betaine and proline betaine by the periplasmic ligand-binding protein ProX from *Escherichia coli*. *J. Biol. Chem.* **2004**, *279*, 5588–5596.
9. Trikha, J.; Theil, E.C.; Allewell, N.M. High resolution crystal structures of amphibian red-cell I ferritin: Potential roles for structural plasticity and solvation in function. *J. Mol. Biol.* **1995**, *248*, 949–967.
10. Schiefner, A.; Holtmann, G.; Diederichs, K.; Welte, W.; Bremer, E. Structural basis for the binding of compatible solutes by ProX from the hyperthermophilic archaeon *Archaeoglobus fulgidus*. *J. Biol. Chem.* **2004**, *279*, 48270–48281.
11. Hitomi, K.; Oyama, T.; Han, S.; Arvai, A.S.; Getzoff, E.D. Tetrameric architecture of the circadian clock protein KaiB. *J. Biol. Chem.* **2005**, *280*, 19127–19135.
12. Horn, C.; Sohn-Bösser, L.; Breed, J.; Welte, W.; Schmitt, L.; Bremer, E. Molecular determinants for substrate specificity of the ligand-binding protein OpuAC from *Bacillus subtilis* for the compatible solutes glycine betaine and proline betaine. *J. Mol. Biol.* **2006**, *357*, 592–606.

13. Wolters, J.C.; Berntsson, R.P.-A.; Gul, N.; Karasawa, A.; Thunnissen, A.-M.W.H.; Slotboom, D.-J.; Poolman, B. Ligand binding and crystal structures of the substrate-binding domain of the ABC transporter OpuA. *PLoS One* **2010**, *5*, doi: 10.1371/journal.pone.0010361.
14. Tschapek, B.; Pittelkow, M.; Sohn-Bösser, L.; Holtmann, G.; Smits, S.H.J.; Gohlke, H.; Bremer, E.; Schmitt, L. Arg149 is involved in switching the low affinity, open state of the binding protein *AfProX* into its high affinity, closed state. *J. Mol. Biol.* **2011**, *411*, 36–52.
15. Du, Y.; Shi, W.-W.; He, Y.-X.; Yang, Y.-H.; Zhou, C.-Z.; Chen, Y. Structures of the substrate-binding protein provide insights into the multiple compatible solute binding specificities of the *Bacillus subtilis* ABC transporter OpuC. *Biochem. J.* **2011**, *436*, 283–289.
16. Marshall, H.; Venkat, M.; Seng, N.S.; Cahn, J.; Juers, D.H. The use of trimethylamine *N*-oxide as a primary precipitating agent and related methylamine osmolytes as cryoprotective agents for macromolecular crystallography. *Acta Cryst.* **2012**, *D68*, 69–81.
17. Ressel, S.; van Scheltinga, A.C.; Vonnrhein, C.; Ott, V.; Ziegler, C. Molecular basis of transport and regulation in the Na<sup>+</sup>/betaine symporter BetP. *Nature* **2009**, *458*, 47–52.
18. Gardberg, A.; Fox, D.; Staker, B.; Stewart, L. *Crystal Structure Of Glycine Betaine, L-Proline ABC Transporter, Glycine/Betaine/L-Proline-Binding Protein (ProX) from Borrelia Burgdorferi*; PDB (Protein Data Bank): Upton, NY, USA, 2013; No. 3TMG.
19. Tan, K.; Shackelford, G.; Joachimiak, A. *The Crystal Structure of A Possible Acetyltransferase Clostridium Difficile 630*; PDB: Upton, NY, USA, 2013; No. 3DSB.
20. Ressler, S.; Scheltinga, A.C.T.V.; Vonnrhein, C.; Ott, V.; Ziegler, C. *Crystal Structure of the Sodium-Coupled Glycine Glutamicum with Bond Substrate*; PDB: Upton, NY, USA, 2013; No. 2WIT.
21. Fujisawa, I.; Takeuchi, D.; Kato, R.; Murayama, K.; Aoki, K. Crystal structures of resorcin[4]arene and tetramethylated resorcin[4]arene complexes incorporating L-carnitine. *Bull. Chem. Soc. Jpn.* **2011**, *84*, 1133–1135.
22. Fujisawa, I.; Takeuchi, D.; Kitamura, Y.; Okamoto, R.; Aoki, K. Crystal structure of an L-carnitine complex with pyrogallol[4]arene. *J. Phys. Conf. Ser.* **2012**, *352*, doi:10.1088/1742-6596/352/1/012043.
23. Murayama, K.; Aoki, K. Molecular recognition involving multiple cation– $\pi$  interactions: The inclusion of the acetylcholine trimethylammonium moiety in resorcin[4]arene. *Chem. Commun.* **1997**, *1*, 119–120.
24. Luostarinen, M.; Åhman, A.; Nissinen, M.; Rissanen, K. Ethyl pyrogall[6]arene and pyrogall[4]arene: Synthesis, structural analysis and derivatization. *Supramol. Chem.* **2004**, *16*, 505–512.
25. Murayama, K.; Aoki, K. Resorcin[4]arene dimer linked by eight water molecules and incorporating a tetraethylammonium ion: guest-driven capsule formation *via* cation– $\pi$  interactions. *Chem. Commun.* **1998**, *5*, 607–608.
26. Mansikkamäki, H.; Nissinen, M.; Schalley, C.A.; Rissanen, K. Self-assembling resorcinarene capsules: Solid and gas phase studies on encapsulation of small alkyl ammonium cations. *New J. Chem.* **2003**, *27*, 88–97.
27. Mäkinen, M.; Vainiotalo, P.; Nissinen, M.; Rissanen, K. Ammonium ion mediated resorcicarene capsules: ESI-FTICRMS study on gas-phase structure and ammonium ion affinity of tetraethyl resorcicarene and its per-methylated derivative. *J. Am. Soc. Mass Spectrom.* **2003**, *14*, 143–151.

28. Aoyama, Y.; Tanaka, Y.; Sugahara, S. Molecular recognition. 5. Molecular recognition of sugars via hydrogen-bonding interaction with a synthetic polyhydroxy macrocycle. *J. Am. Chem. Soc.* **1989**, *111*, 5397–5404.
29. Sheldrick, G.M. A short history of SHELX. *Acta Cryst.* **2008**, *A64*, 112–122.
30. Kabuto, C.; Akine, S.; Nemoto, T.; Kwon, E. Release of software (Yadokari-XG 2009) for crystal structure analyses. *J. Cryst. Soc. Jpn.* **2009**, *51*, 218–224.
31. Farrugia, L.J. ORTEP-3 for windows—A version of ORTEP-III with a graphical user interface (GUI). *J. Appl. Cryst.* **1997**, *30*, 565.
32. CCDC CIF Depository Request Form for data published from 1994. Available online: <http://www.ccdc.cam.ac.uk/conts/retrieving.html> (accessed on 7 April 2013)

© 2013 by the authors; licensee MDPI, Basel, Switzerland. This article is an open access article distributed under the terms and conditions of the Creative Commons Attribution license (<http://creativecommons.org/licenses/by/3.0/>).